(Preprint) AAS 12-005

ANALYSIS OF THE TOUCH-AND-GO SURFACE SAMPLING CONCEPT FOR COMET SAMPLE RETURN MISSIONS

Milan Mandić, Behçet Açıkmeşe, David S. Bayard, and Lars Blackmore *

This paper studies the Touch-and-Go (TAG) concept for enabling a spacecraft to take a sample from the surface of a small primitive body, such as an asteroid or comet. The idea behind the TAG concept is to let the spacecraft descend to the surface, make contact with the surface for several seconds, and then ascend to a safe location. Sampling would be accomplished by an end-effector that is active during the few seconds of surface contact. The TAG event is one of the most critical events in a primitive body sample-return mission. The purpose of this study is to evaluate the dynamic behavior of a representative spacecraft during the TAG event, i.e., immediately prior, during, and after surface contact of the sampler. The study evaluates the sample-collection performance of the proposed sampling end-effector, in this case a brushwheel sampler, while acquiring material from the surface during the contact. A main result of the study is a guidance and control (G&C) validation of the overall TAG concept, in addition to specific contributions to demonstrating the effectiveness of using nonlinear clutch mechanisms in the sampling arm joints, and increasing the length of the sampling arms to improve robustness.

INTRODUCTION

Spacecraft exploration over the last decade has been expanding in many new directions. One important direction is the exploration of primitive bodies such as asteroids and comets, and surface proximity operations. Recent missions include the Deep Space 1 mission that flew-by the comet Borrelly,[1] the Near Earth Asteroid Rendezvous (NEAR) mission that orbited and eventually landed on the asteroid Eros,[2] the 2004 Stardust mission that flew through the dust field of comet Wild 2,[3] and the Deep Impact mission that drove an impactor at high velocity into comet Tempel 1.[4] Challenging missions include the Japanese Hayabusa mission (formerly MUSES–C) launched in 2003 that touched down two times on asteroid Itokawa and returned back to Earth in 2010 with small amount of collected samples of asteroidal material,[5, 6] and the European Rosetta mission[7] launched in 2004 and scheduled to orbit and land on comet 67P/Churyumov–Gerasimenko in 2014.

An important component of exploring primitive bodies is the ability to take a surface sample. This paper studies the Touch-and-Go (TAG) concept for enabling a spacecraft to take a sample from the surface of the primitive body. The idea behind TAG is to let the spacecraft descend to the surface, make contact with the surface for several seconds, and then ascend to a safe location. Sampling would be performed by an end-effector that would be active during the few seconds of surface contact.

* Jet Propulsion Laboratory, California Institute of Technology, mandic@jpl.nasa.gov, acikmese@jpl.nasa.gov, bayard@jpl.nasa.gov, larsb@mit.edu. © 2012 California Institute of Technology. Government sponsorship acknowledged.

The TAG concept avoids having to separately land and anchor to the surface before sampling, and then unanchor prior to leaving the surface. Furthermore, TAG would provide the surface-normal-forces needed for sampling by using the inertia of the descending spacecraft, rather than requiring downward thrusting which could be dangerous in close surface proximity, or the risks of getting stuck from using pyro-driven harpoon-like mechanisms. The TAG event would be one of the most critical events in a primitive body sample-return mission. The purpose of this TAG study is to evaluate the dynamic behavior of a representative spacecraft during the TAG event, i.e., immediately prior, during and after the surface contact of the sampler. Moreover, the study evaluates the sample-collection performance of the proposed sampler, in this case a brush wheel sampler, for acquiring surface material during contact.

There are many challenges surrounding the surface proximity operations necessary to implement a TAG maneuver for primitive body sample return. Two-way communication flight times on the order of an hour or more would require the spacecraft to operate in close proximity to the comet surface for long periods of time, without the benefit of Earth ground-command interaction. This requirement drives the need for on-board autonomy. In addition, autonomous navigation based on terrain-relative navigation must be performed to establish spacecraft position and velocity relative to the comet surface, and autonomous guidance must be performed to bring the spacecraft down along a specified path to the desired sampling site. During the sampling event, a specific guidance condition (i.e., surface-relative velocity, orientation, and contact duration) must be maintained to ensure that a sufficient sample is obtained. After sampling, the spacecraft must remove rates induced from sampling-induced reaction forces, and then execute a thruster-based maneuver to ascend from the comet surface.

This paper focuses on the sampling/TAG event and summarizes results of the simulated TAG scenarios for a potential representative comet sampling mission. It also provides information about the potential spacecraft configuration, surface properties and mission parameters. The study is based on using the G-TAG software[8] that was developed under a NASA-JPL R&D program on Integrated Autonomous Guidance, Navigation and Control for a Comet Sample Return.[9] G-TAG represents a novel multi-body dynamics simulation software tool, designed to simulate a TAG maneuver for sampling from the surface of a primitive body. This software utilizes a multi-body simulation engine, G-DYN,[10] and has interfaces to controllers[11] and environmental forces that would affect the spacecraft. The G-TAG analysis and simulation tool will be briefly described in the paper. Results are visualized using the G-View software,[12] which has also been developed under the NASA-JPL R&D program, which creates movies of the simulation runs, with example visualizations depicted in the snap-shots of Figures 1 and 2.

In order to demonstrate the feasibility of the TAG concept, analysis is needed to validate that key requirements would be met by the spacecraft design configuration. These requirements include: (i) Providing sufficient contact force and duration to ensure that enough surface material would be collected; (ii) Providing survivability of the spacecraft from the contact event, i.e., ensuring that no part of the spacecraft (besides the sampling mechanism) would come into contact with the surface; (iii) Recovering from induced sampling disturbances and ascending to a safe position, velocity, and orientation.

In order to evaluate whether requirements are satisfied, spacecraft TAG dynamics are simulated and the following variables are computed: (i) The contact force as a function of time; (ii) The surface relative states of the spacecraft components, such as, solar panels; (iii) The dynamic state of the spacecraft bus. The simulated performance of the proposed spacecraft during TAG is evaluated

based on metrics representing survivability, sample collection performance, and antenna pointing accuracy. Scenarios consider sensitivity to the ground slope and the surface properties, as well as various spacecraft design characteristics.

TAG CONCEPT PROPERTIES AND MODELING

This section describes some of the most relevant items of the TAG concept, such as the spacecraft configuration, surface properties and other parameters. Each of these parameters has an effect on the overall performance of the sampling system.

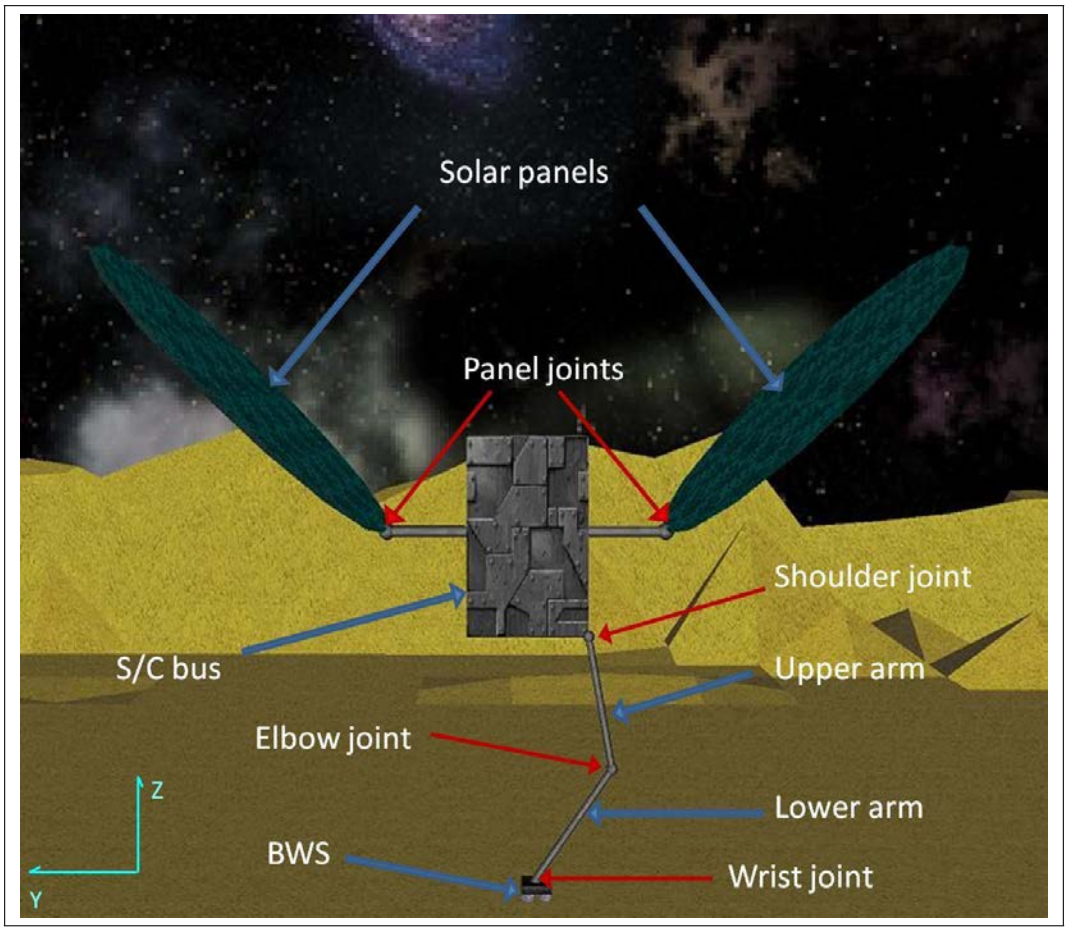

Figure 1. Comet spacecraft, visualized using G-View software. Red arrows point to joints, blue arrows to spacecraft body components. The G-TAG frame used for the simulation and for creating simulation movies is shown in the lower-left corner. X-axis completes coordinate system using the right-hand rule.

Reference Spacecraft Configuration

The representative spacecraft configuration for the comet touch-and-go concept is shown in Figure 1. The spacecraft would consist of spacecraft bus, two solar panels, upper and lower sampling arms, and the brush-wheel sampler (BWS) used to collect the sample during the TAG event. Each of the spacecraft components, i.e., *bodies*, is represented as a rigid body. Model also includes various

thruster types, which generate external forces on the spacecraft bus. A sample scenario mass and inertia values for the spacecraft components are provided in Table 1.

Table 1. Assumed mass and inertia properties of spacecraft configuration components

Spacecraft component	Mass (kg)	Size	Inertia (kgm^2)
Bus	2200	$2.085 \times 2.085 \times 3.416\, m^3$	$I_x = 2896.3$; $I_y = 2896.3$; $I_z = 1572.2$
Panel 1	100	8.1 m (diameter)	$I_x = 2152.8$ $I_y = 430.6$ $I_z = 430.6$
Panel 2	100	8.1 m (diameter)	$I_x = 2152.8$ $I_y = 430.6$ $I_z = 430.6$
Upper Arm	7.5	2.3 m (length); 0.1 m (diameter)	$I_x = 10.13$ $I_y = 10.13$ $I_z = 0.0094$
Lower Arm	7.5	2.3 m (length); 0.1 m (diameter)	$I_x = 10.13$ $I_y = 10.13$ $I_z = 0.0094$
BWS	5	$0.5 \times 0.2 \times 0.5\, m^3$	$I_x = 0.12$ $I_y = 0.12$ $I_z = 0.20$

The two solar panels would have a 45° x-axis cant angle. This cant angle would be used during the TAG event to decrease the chances of panel contact with the comet surface during the TAG event. The panel joints are modeled as the pin-joints, i.e., the panels are constrained in two rotational directions and free to rotate in only one (x-axis). The x-axis rotational dynamics is represented with spring-damper system:

$$I_{xx}\ddot{\theta}_x + 2\omega_x\zeta\dot{\theta}_x + \omega_x^2\theta_x = 0 \tag{1}$$

where $\zeta = 2\%$ is the damping coefficient and $\omega_x = 2\pi f_x$ with $f_x = 0.6Hz$ the natural frequency of the panel joint, while $I_{xx}\ddot{\theta}_x = \tau_{panel}$ is the external torque on the panel joint.

The two arms, upper and lower, are attached to each other with an elbow joint, represented as the nonlinear clutch damping pin-joint. Similarly, the upper arm is connected to the spacecraft bus with the identical nonlinear clutch damping pin-joint. The lower arm is rotated 30° degrees from vertical axis (z-axis), while the upper arm is under an angle of 5° from vertical, as shown in Figure 1. These two joints are critical elements in determining the sampling force profile, used for satisfying one of the sampling requirements. The profile and description of the nonlinear clutch damping joints is in Clutch Torque Section.

The BWS is connected to the lower arm with a wrist joint. For the comet scenario, the wrist joint has been locked in order to avoid the “flipping” of the BWS, Figure 2, which can occur due to the center-of-rotation of the joint being above the BWS, and to allow for the BWS to “dig” into the softer comet surface, if necessary.

The representative spacecraft configuration includes thrusters of various thrust and type. For this set of simulations, the spacecraft model is equipped with 16 thrusters: four 200N cold-gas thrusters and 12 hydrazine thrusters with multiple thrust values. However, the hydrazine thrusters are kept turned-off during the TAG event to prevent contamination. During the descent stage, for the last 40 meters of the approach, all thrusters are turned off. Therefore, there is no control actuation during the immediate descent stage and during the sampling thruster-free stage (1.5 seconds). After the sampling thruster-free stage expires, the cold-gas thrusters are turned on to ascent and recover the spacecraft attitude and altitude. The cold-gas thrusters have a cant angle requirement of 45° away from the edge of the spacecraft bus. The thruster cant angle requirement would assure there is no

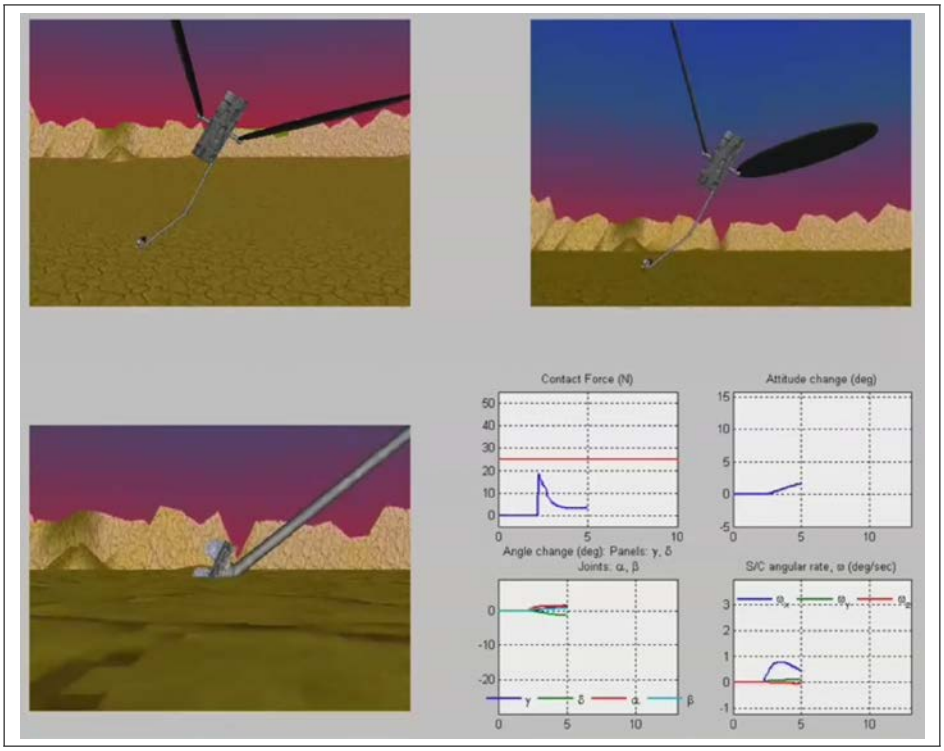

Figure 2. Sample scenario showing the BWS flipping over - see bottom-left screenshot. Image is a snapshot of the G-View movie, created using the data generated by G-TAG simulation software. This scenario shows an earlier version of the spacecraft.

pluming or physical disturbance of the landing site area during the ascent stage, thus allowing the science team to return to the same location for another sampling.

Surface Properties

The surface of the comet is modeled as a spring-damper system,[13]

$$F_{vertical} = -k_s p_{bw_i} - c_s v_{bw_{ni}} \tag{2}$$

with $F_{vertical}$ as the vertical force applied on the brush wheels of the BWS and where p_{bw_i} and $v_{bw_{ni}}$ are the vertical position and normal component of the velocity of the brush wheel $\boldsymbol{i}$ with respect to the comet's surface, respectively, as seen in the left schematics of the Figure 3. This setup allows for adjusting the "softness" and "hardness" of the surface and for examining the performance of the spacecraft and BWS in these situations. The opposite, downward force from spacecraft upon the comet surface is a function of the spacecraft dynamics. This value is used for computing the normal force responsible for the sampling. The typical surface values used for the simulation scenarios are:

- *soft*: with stiffness coefficient $k_s = 20Nm/^\circ$ and damping coefficient $c_s = 0.5Nms/^\circ$
- *hard*: with stiffness coefficient $k_s = 100Nm/^\circ$ and damping coefficient $c_s = 0.5Nms/^\circ$

The lateral friction component of the contact model is formulated as simple kinetic friction for the BWS dragging across the surface at a lateral velocity, as illustrated in right schematics of the

Figure 3. The kinetic friction is given by

$$F_{friction} = \mu_k N \tag{3}$$

where μ_k is the coefficient of kinetic friction for the surface material and N is the normal force reacting to the spacecraft contacting the surface. The normal force is $N = F_{vertical}$ from Equation 2.

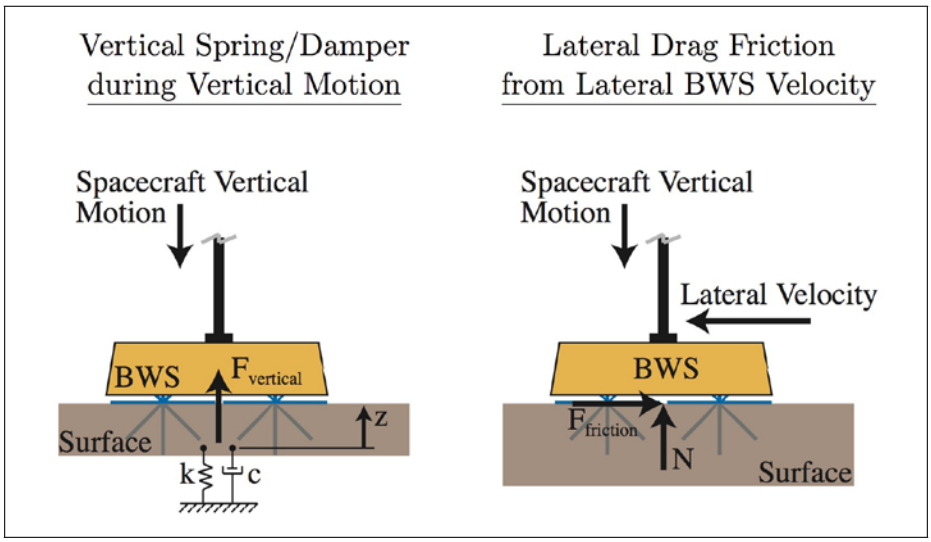

Figure 3. Forces on the BWS: Left - vertical force and the spring-damper model of the surface; Right - horizontal, friction force

Gravity model

The gravity model consists of the gravitational attraction of the Sun and the comet. Gravitational fields from other sources are negligible and not included in the gravity model. The total gravitational acceleration of the spacecraft is then computed as:

$$g_{total} = g_{sun} + g_{comet} \tag{4}$$

where $g_{sun} = \mu_{sun} \frac{\hat{r}_{sun}}{|r_{sun}|^2}$ and $g_{comet} = \mu^{comet} \frac{\hat{r}_{comet}}{|r_{comet}|^2}$. The $\mu_{sun} = 132 \times 10^9 (km^3/s^2)$ and $\mu_{comet} \approx 6.67 \times 10^{-8} (km^3/s^2)$ are the gravitational constants. The value for μ_{comet} is based on an assumption for the comet mass, $m_{comet} = 10^{12} kg$, which is used for the simulations. The $\hat{r}_{sun}$ and $\hat{r}_{comet}$ are the unit vectors corresponding to r_{sun} and r_{comet} respectively, which represent the position of the spacecraft with respect to the center of gravity of the sun and comet.

Clutch Torque

The shoulder and elbow joints use a nonlinear clutch torque system, Figure 4. The torques in these two joints would be identical and supplied by a nonlinear damper that approximates a clutch that provides pure coulomb friction. The two joints have a single degree of freedom, each defined about the x-axis of the upper arm (for the shoulder joint) and the lower arm (for the elbow joint). The x-axis for the shoulder and elbow joints are defined by the initial body frame of the upper and lower arm, respectively. The values of the break location, $\Delta\omega_1$, and Max clutch torque in Figure 4, can be adjusted to achieve the desired sampling contact force profile. The tail-slopes are usually kept at zero.

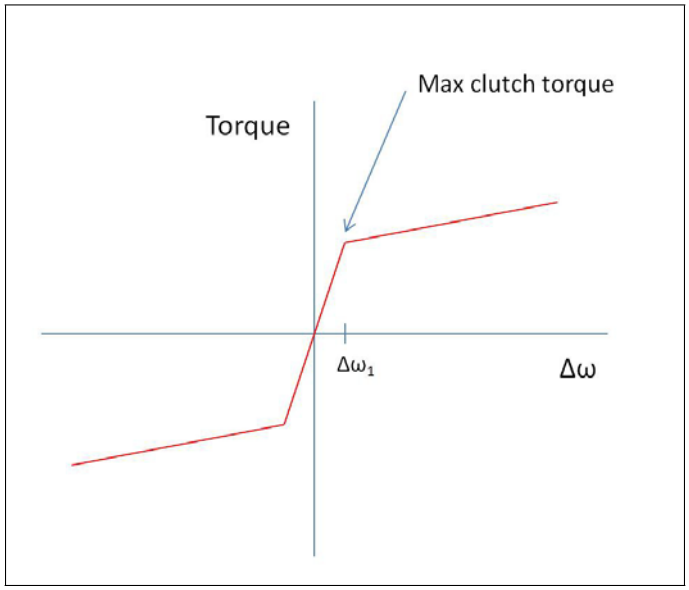

Figure 4. Nonlinear clutch torque profile for the shoulder and elbow joints

GTAG SOFTWARE DESCRIPTION

The TAG event would be by far the most risky of all proximity operations, and the one that is in the main spotlight when designing small body sampling missions. Therefore, there is a clear need for an analysis tool to help understand the TAG event. In order to fill this need, G-TAG software was developed as part of the R&D effort.[8] The main purpose of the G-TAG tool is to provide a flexible and fast turn-around simulation tool to validate the TAG methodology, help to size TAG components, set requirements, and answer the many what-ifs that arise associated with the TAG event. G-TAG is a simulation test environment developed in Matlab, and specifically designed to simulate the time interval just prior to TAG (while the S/C is descending), during TAG (contact with surface), and then the period immediately following TAG (S/C ascent). G-TAG leverages the primal-dual formulation of the dynamics used in the G-DYN dynamics software engine,[10] where G-DYN is a simulation engine/algorithm for multi-body dynamics of rigid body dynamics, which powers the G-TAG software. In other words, G-TAG can be described as a wrapper for the G-DYN engine, as shown in Figure 5. The wrapper is used to setup the software interface, and to facilitate the user with the simulation environment.

The first block in the Figure 5 defines the integration algorithm and the control frequency. Integration step can be fixed, or adaptive, depending on which integration algorithm is chosen (i.e. Matlab functions: ode4, ode5, ode45 etc).

The second set of four blocks in Figure 5 consists of the following:

- Definition of initial conditions
- Preparation of the information to be processed, converting all the necessary data in appropriate frames and units
- Definition of the multi-body system (i.e., spacecraft) geometry, with locations, masses, inertias and other relevant information about the components. Primal-dual dependencies and

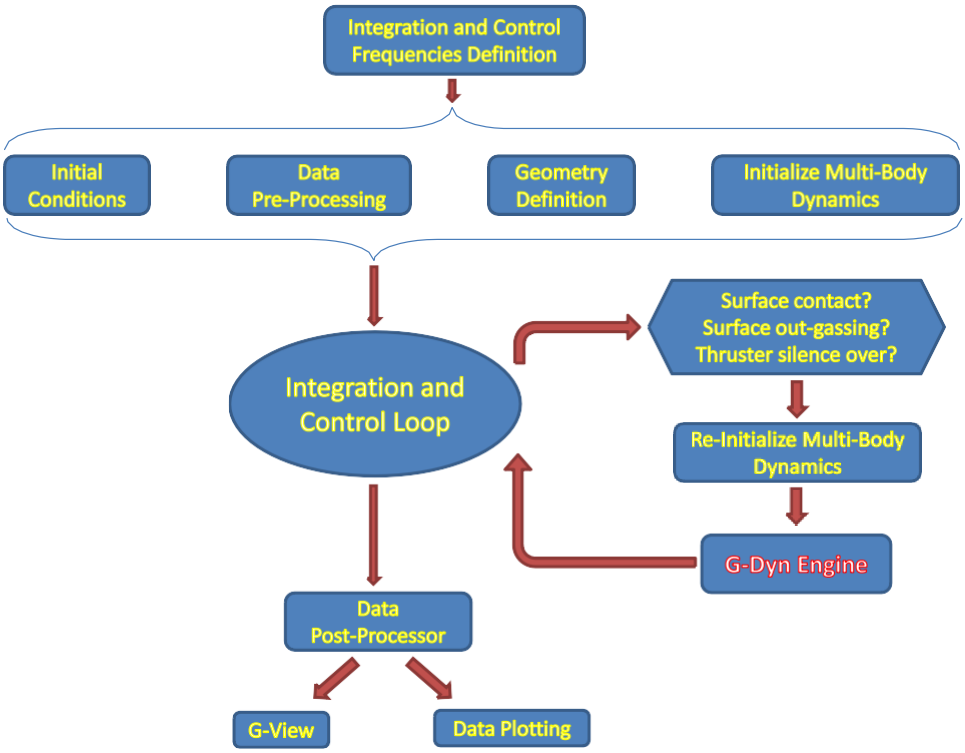

Figure 5. Flow chart for G-TAG simulation software

joint properties are also defined here, such as translational and rotational degrees of freedom, torsional models (i.e., spring-damper model)

- Initialization of the multi-body dynamics, setting up relative initial conditions for multi-body model, specifying the equilibrium states of spacecraft components.

Once all the necessary information is arranged, the algorithm begins the simulation loop. At each integration step all the forces and torques acting on spacecraft components and joints are calculated. In addition to gravity, the simulation detects if any additional external forces are present, as they are not present at all times. For example, the normal and friction forces due to the contact with the small body surface, disturbance forces from comet out-gassing, and forces due to thruster firing are not acting upon the spacecraft configuration at all times. Once these values are computed, they are processed using the G-DYN engine for the next integration step. Also, within the integration loop a control algorithm and a thruster allocator are incorporated, thus allowing the user to test different ascent control algorithms and optimization schemes for fuel consumption etc.

Finally, once the numerical integration is completed, outputs are post-processed by mapping states and parameters into their desired frames.

Multi-body Dynamics Software, G-DYN

As noted earlier, G-DYN is a simulation engine for multi-body dynamics of rigid body dynamics, which powers the G-TAG software. The G-DYN formulation considers the translational and rotational velocities (primal variables) and the interaction forces and torques (dual variables) as solution variables. This method is different than the Lagrangian approach where the independent degrees-of-freedom of the system are considered as solution variables. Hence the solution vector is of larger dimension in the primal-dual formulation. However, this comes with some major advantages: (i) The ease of formulation of equations of motion for multi-body systems, and the automation of this process. (ii) The computation of interaction forces and torques, which is useful in some engineering applications, specifically in touch-and-go sampling of small body surfaces. (iii) The components in a model can easily be replaced by new ones, i.e., *interchangeability*, or their interconnections can be rearranged, i.e., *reconfigurability*, in an automated fashion. (iv) Component-wise model reduction can be performed. (v) Rigid and flexible bodies can be analyzed in a single framework. (vi) The equations of motion have a transparent sparse structure as a function of the interconnection topology, which can be exploited for efficient computations.

TAG PERFORMANCE MEASURES

G-TAG simulations are used to study the sensitivity of performance measures to changes in the spacecraft and comet surface elements, such as the thruster force levels and their cant angles, the surface properties, ground slope, drop velocities, etc. The main performance measures are survivability, sample collection performance, and antenna pointing accuracy. Each of these measures are essential for mission success. The survivability criterion is perhaps the most critical, since the mission concept allows for several attempts at collecting the sample. The performance criteria are defined as follows:

Sampling: Contact force and duration must be sufficient to ensure that enough surface material is collected;

Sample collection performance is measured by the contact force profile established between the brush wheels of the BWS and the comet surface. The required contact force level is at least $2N$ with desired level of $5N$, with a contact time greater than 1.5 seconds. This criterion mainly depends on the joint properties of the sampling arms, surface properties and descent velocity.

Survivability: The spacecraft must survive the contact event, i.e., no part of the spacecraft (besides the sampling mechanism) would come into contact with the surface.

Survivability is measured as the maximum allowable thruster silence-time delay. This is the maximum thruster-silence time duration that the spacecraft can command after contact with the surface before it must fire its thrusters in order to avoid an impact. Here an impact is defined as surface contact with any part of the spacecraft other than the sampling device. The most informative cases are the extreme limiting scenarios, for example cases with a 45° surface inclination angle. A metric used for characterizing spacecraft safety is the closest distance that the elbow joint and solar panel come to the comet surface during the TAG event. For this study, closest approach distances greater than one meter are considered acceptable.

Recoverability: The spacecraft must be able to recover and ascend to a safe position, velocity, and orientation.

Spacecraft attitude errors during TAG can be assessed by looking at the antenna pointing accu-

racy. Antenna pointing is measured by the total rotation angle from a fixed inertial reference point, where the reference point is defined as the initial attitude of the spacecraft bus. Antenna pointing is required to maintain spacecraft communication with Earth ground control during mission critical stages, such as descent and the TAG event. The maximum allowable pointing error is estimated at around $\pm 20^\circ$.

SIMULATION

TAG Parameters

TAG parameters are established to account for various TAG configurations. These parameters are meant to cover a large test space for performance evaluation of the spacecraft configuration during the TAG event and thus provide high model fidelity and reliability. Parameters used in the simulations mainly represent an envelope of the possible scenarios, or the worst case scenarios. For this paper, the spacecraft bus, panels, BWS, thrusters, controller and thruster allocator properties are kept fixed, as they were derived from extensive testing and prior consideration of representative mission constraints.

One such parameter is contact or drop velocity, i.e., the vertical descent velocity along the *z*-axis of the spacecraft bus body frame, as in Figure 1. As mentioned earlier, active control of the spacecraft is assumed to be terminated at an altitude of 40m above comet surface, in anticipation of the TAG event. In order to account for possible drop velocity variations due to the potential estimation errors and modeling uncertainties, the simulations cover the envelope drop velocities, i.e., the minimum and maximum expected. These variations have an effect on the contact duration and contact force profile, as well on the survivability. The minimum expected drop velocity is fixed at v_d (*min*) = 0.19*m/s* while the maximum drop velocity is set at v_d (*max*) = 0.21*m/s*.

Similarly to drop velocity, another TAG parameter is the horizontal velocity, i.e., velocity in the directions parallel to the comet surface plane. In this case, the selected values for the horizontal velocity may also be the result of the estimation and modeling errors. The nominal value is fixed to be at v_h (*nominal*) = 0*m/s*, while the maximum is set at v_h (*max*) = 0.06*m/s*.

Ground slope at contact is another important TAG parameter. Variations in slope could also affect contact duration, and therefore the contact force profile. If the slope is considered over a wider landing area, such as the slope of a local hill or valley on the comet, rather than just over the immediate landing spot of the BWS, then the ground slope would have a major effect on the survivability of the spacecraft. Larger slopes would not only cause the elbow and the solar panel to come closer to the surface during TAG, but would also induce higher rotational rates following the contact, due to the longer rotation arm from the center of mass of the spacecraft. The nominal slope is set at 0°, with worst case scenario fixed at 45°.

In order to test how long it takes the spacecraft to have an undesired impact with the comet surface, the commanded thruster silence time could be varied. The danger of impact is conveniently quantified by the time it takes for the spacecraft to make a contact with surface with any part of the spacecraft other than the BWS. As the simulations for spacecraft depicted in Figure 1 show, this means contact between the surface and either the elbow joint or the solar panel tip. The commanded thruster silence time effects both the contact force profile, the spacecraft attitude, and ultimately the spacecraft survivability. In the nominal case the commanded thruster-silence time is set at t_s = 1.5*sec*.

Finally, the length of the sampling arms is varied in the model. The nominal value of both arms is set at 2.3*m*. In order to improve spacecraft safety during surface contact, the simulations are also performed with 75% longer upper and lower sampling arms, at 4.025*m* each. Results indicate that elongation has both positive and negative effects on sampling performance. The situation is improved further by adjusting the nonlinear clutch torques.

Simulation Results

Simulation results are summarized in the format presented in Figures 6, 8. Selected scenarios cover the most relevant range of values, but for this study, do not cover combinations of all the parameters. For example, the horizontal velocity is only used in the nominal cases, to indicate if there are any significant perturbations due to the horizontal velocity. Nominal cases are defined as the 0° surface inclination at the landing spot. Figures are divided in two sections - the TAG Simulation Parameters section, and the Results section. Relevant parameters have already been described earlier in more detail. In the Results section of the figures, there are several columns representing spacecraft performance.

The first column of results is the contact force time duration. The values in this column indicate the amount of time in seconds during which the BWS has established the contact force greater than 2*N* and 5*N*. This is dependent on the thruster delay time before ascent, which is fixed at 1.5*sec*, shown in column six of the Simulation Parameters section of the figures . After this delay the spacecraft is still in contact with the surface, extending the sample collection time for a certain duration, until the thrusters raise the BWS above the ground.

The second and third columns indicate the closest approach of elbow joint and the tip of the panel to the surface, respectively. These values need to have a reasonable margin, in order to indicate safe approach. Scenarios that have a relatively close approach for either of the two values, are deemed unsafe and may require changes in the spacecraft and TAG design.

Finally, the fourth column indicates the total rotation of the spacecraft, simply called the antenna pointing offset. This value needs to remain within 20° to ensure the accurate pointing to the ground communication stations. This also serves as measure of spacecraft recoverability from sampling-induced reaction forces, and it is computed as the rotation angle around a general axis derived from the quaternion of the spacecraft bus.

Figure 6 shows the performance of the spacecraft configuration with an upper and lower arm length of 2.3*m*. In this set of simulations the maximum value of nonlinear clutch torque from Figure 4 is set at 30*Nm*. The simulations show that the small horizontal velocity in nominal cases does not have a significant impact on spacecraft performance.

In nominal cases, the contact time is about four seconds for a soft surface and about three seconds for a hard surface, for both 2*N* and 5*N* markers, which can be considered as a sufficient collection time for the BWS end-effector. However, when the surface is inclined by 45°, referred to as a stress case, the 5*N* contact time decreases to only about the 1.5*sec* corresponding to the thruster silence time before ascent, and can still be considered sufficient to collect enough sample. On the other hand, the closest approach to the surface of the elbow is only about 0.5 meters which can be deemed unsafe per requirements. One possible method to address this issue is to test the performance of the reference spacecraft with elongated arms. For this purpose, an increase of 75% in length for both upper and lower arms is considered, or, equivalently, to 4.025*m* each. The last two simulation scenarios in Figure 6 show the approximate longest thruster silence time before ascent that will still

avoid spacecraft-surface impact. As seen in these two scenarios, it is the elbow joint that first comes into contact with the surface of the comet if the commanded thruster silence time before ascent is increased to more than 7 seconds.

SIMULATION PARAMETERS							RESULTS			
Case		Surf ace	Slope (deg)	Horiz. Vel. (m/s)	Drop velocity (m/s)	Delay before ascent (s)	2N/5N Contact Time (s)	Closest approach Elbow (m)	Closest approach Panel (m)	Antenna PoinNng offset (°)
NOMINAL	1	S	0	0.06	0.19	1.5	4.14/3.81	1.73	10.78	0.84
	2	S	0	0.06	0.21	1.5	4.17/3.87	1.67	10.73	0.78
	3	H	0	0.06	0.19	1.5	3.21/3.03	1.73	10.78	0.84
	4	H	0	0.06	0.21	1.5	3.26/2.77	1.67	10.73	0.82
STRESS	5	S	45	0	0.19	1.5	3.02/1.63	0.48	2.3	1.84
	6	S	45	0	0.21	1.5	3.15/1.84	0.46	2.27	1.98
	7	H	45	0	0.19	1.5	2.56/1.57	0.53	2.23	1.86
	8	H	45	0	0.21	1.5	2.68/1.66	0.55	2.25	1.90
	9	S	45	0	0.21	7	8.05/6.61	~0	0.95	7
	10	H	45	0	0.21	7	7.64/6.38	~0	0.90	7

Figure 6. The simulation results with 2.3*m* **upper and lower arm length. "S" stand for soft surface, and "H" stands for hard surface.**

As an example showing simulation plots from the G-TAG tool, Figure 7 shows quantities corresponding to Case 1 of the short-arm configuration from Figure 6. In addition to the aforementioned contact force profile, the elbow and panel closest approach and antenna pointing graphs, the plots also show the angular rates, velocities and cumulative ΔV which is indicative of fuel consumption. The cumulative ΔV graph also shows that the thrusters start firing at about 4.5 seconds, or 1.5 seconds after the initial contact is established, as shown in the contact force subplot, which corresponds to the thruster delay time of 1.5 seconds. The half rotation angle subplot represents the half-angle of the total rotation around the spacecraft rotation axis, as computed from the attitude quaternion of the spacecraft bus.

Figure 8 shows simulation results for the case where the upper and lower arms are 75% longer. Again, the horizontal velocity does not have significant effect. However, the elbow and panel closest approach values are much improved, as expected. These scenarios can now all be deemed safe, as no part of the spacecraft gets closer than 1 meter from the surface. The last two cases show that the commanded thruster silence time before ascent can be extended to approximately 17 seconds and still avoid a S/C-surface impact. With longer arms, such a surface contact would first be made with the solar panel tip, in contrast to the short-arm cases where contact would first be made with the elbow. On the other hand, the contact force durations for the stress cases are not satisfactory. Some stress cases have 5*N* contact times significantly less than 1 seconds, while 2*N* marks are attained for only a duration of thruster silence time. Therefore, even though the long-arm scenarios show improved safety during the contact with surface, the BWS is not collecting sufficient amount of the material.

In order to improve the BWS sample collection times, another adjustment is made to the long-arm spacecraft configuration. In this case, the modification is done on the elbow and shoulder joints,

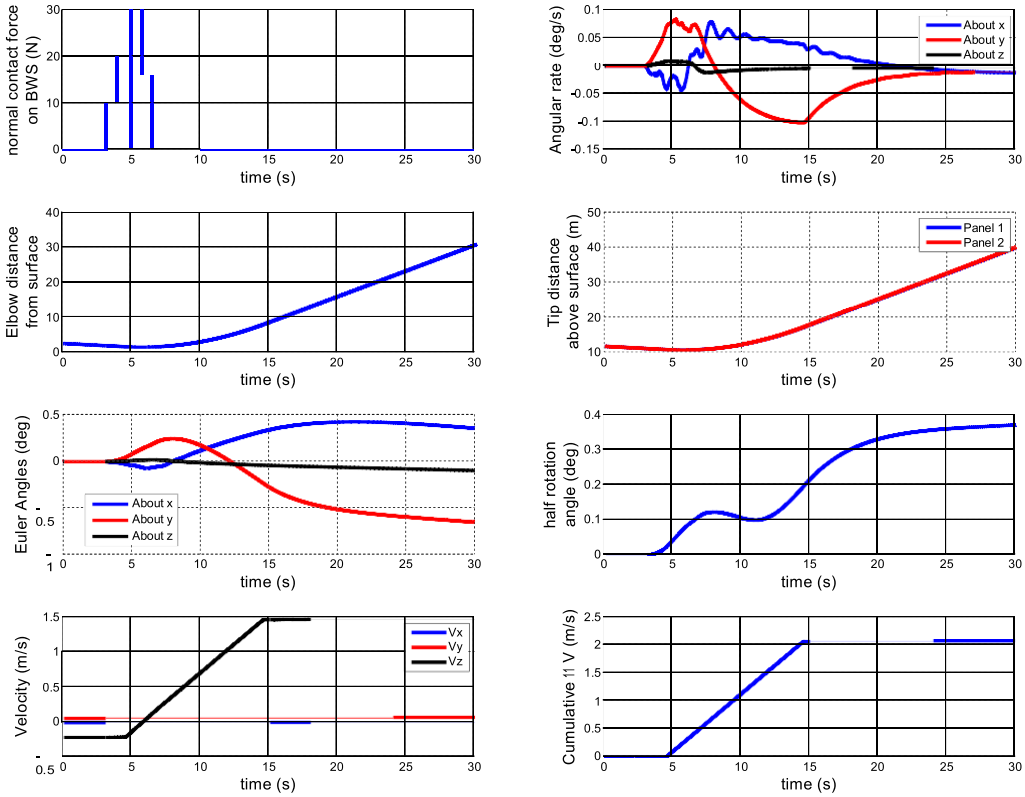

Figure 7. Simulation plots for Case 1 of Figure 7 for the spacecraft configuration having 2.3*m* upper and lower arm lengths.

by increasing their maximum clutch torque to 80*Nm*. This value provides an increased sampling force against the surface, and acts to increase contact times. Simulations have shown that closest approach margins remain large enough - very similar to the results in Figure 8, thus preserving the safety of the spacecraft. In addition, Table 2 shows the improvement of the contact times for the 2*N* and 5*N* contact force levels. These contact times are comparable with the contact times seen from the spacecraft configuration with shorter (2.3*m*) arms, Figure 6.

An important conclusion from the study follows from summarizing the previous case where *the synergistic effect of increasing arm lengths and re-stiffening the nonlinear clutches in the arm joints provides a spacecraft configuration that combines the benefits of having a sufficient contact force and time duration for sample collection, while maintaining safe distance between the other spacecraft components and the comet's surface*. Aside from serving as an important conclusion from the study, the result underscores the general usefulness of the G-TAG tool for performing comparative analysis of candidate TAG configurations.

CONCLUSION

This study provides a G&C validation of the overall TAG concept for primitive body surface sample acquisition by simulating performance of a representative spacecraft during the TAG event, and evaluating metrics representing survivability, sample collection performance, and antenna pointing accuracy. Scenarios consider sensitivity to the ground slope and the surface properties, as well

SIMULATION PARAMETERS							RESULTS			
Case		Surf ace	Slope (deg)	Horiz. Vel. (m/s)	Drop velocity (m/s)	Delay before ascent (s)	2N/5N Contact Time (s)	Closest approach Elbow (m)	Closest approach Panel (m)	Antenna PoinNng offset (°)
NOMINAL	1	S	0	0.06	0.19	1.5	3.12/2.76	4.04	13.96	0.96
	2	S	0	0.06	0.21	1.5	3.23/2.82	3.99	13.92	0.94
	3	H	0	0.06	0.19	1.5	2.44/1.63	4.04	13.96	0.88
	4	H	0	0.06	0.21	1.5	2.53/1.81	3.99	13.91	0.86
STRESS	5	S	45	0	0.19	1.5	1.99/0.69	1.56	4.03	1.50
	6	S	45	0	0.21	1.5	2.38/0.0	1.53	4.00	1.58
	7	H	45	0	0.19	1.5	1.24/0.70	1.57	4.02	1.46
	8	H	45	0	0.21	1.5	1.60/0.74	1.54	3.98	1.52
	9	S	45	0	0.21	17	5.82/0.0	0.15	~0	13
	10	H	45	0	0.21	17	4.93/0.72	0.16	~0	13

Figure 8. The simulation results with $4.025m$ **upper and lower arm length."S" stand for soft surface, and "H" stands for hard surface.**

Table 2. Contact time (in seconds) for the reference spacecraft configuration with elongated upper and lower arms and with increased maximum clutch torque (defined in Figure 4) to $80Nm$**. The case numbering follows the ones in Figures 6, 8.**

Case	1	2	3	4	5	6	7	8
$2N/5N$ Contact time (s)	4.19/3.86	4.4/4.1	3.22/3.08	3.15/2.93	2.79/1.47	2.94/1.77	2.28/1.89	2.32/1.96

as various spacecraft design characteristics. In addition to validating the basic TAG methodology, study results also indicate the effectiveness of using a nonlinear clutch mechanism in the sampling arm joints, and demonstrate the benefits of increasing the length of the sampling arms to improve samplingrobustness.

All simulations are performed using the G-TAG analysis and simulation software tool, developed under the NASA-JPL Research & Technology Development program. Results indicate that G-TAG can serve as a useful G& C analysis tool for validating candidate TAG approaches for emerging primitive body missions.

ACKNOWLEDGMENTS

This research was performed at the Jet Propulsion Laboratory, California Institute of Technology, under contract with the National Aeronautics and Space Administration.

REFERENCES

[1] S. Bhaskaran, J. Riedel, B. Kennedy, and T. Wang, "Navigation of the Deep Space 1 Spacecraft at Borrelly," *AIAA 2002-4815, AIAA/AAS Astrodynamics Specialists Conference*, 2002.

[2] W. Owen and T. Wang, "NEAR Optical Navigation at Eros," *AAS 01-376, AAS/AIAA Astrodynamics Specialists Conference*, 2001.

[3] S. Bhaskaran, J. Riedel, and S. Synnott, "Autonomous Nucleus Tracking for Comet/Asteroid Encounters: The STARDUST Example," *IEEE Aerospace Conference Proceedings*, Vol. 2, 1998, pp. 353–365.

[4] D. Kubitschek, "Impactor Spacecraft Targeting for the Deep Impact Mission to Comet Tempel 1," *AAS 03-615, AAS/AIAA Astrodynamics Specialists Conference, Big Sky Resort, Big Sky, Montana*, 2003.

[5] T. Kubota, T. Hashimoto, J. Kawaguchi, M. Uo, and K. Shirakawa, "Guidance and navigation of the Hayabusa spacecraft for asteroid exploration and sample return mission," *SICE-ICASE, Busan, Korea*, 2006, pp. 2793–2796.

[6] T. Nakamura, T. Noguchi, M. Tanaka, M. E. Zolensky, M. Kimura, A. Tsuchiyama, A. Nakato, T. Ogami, H. Ishida, M. Uesugi, T. Yada, K. Shirai, A. Fujimura, R. Okazaki, S. A. Sandford, Y. Ishibashi, M. Abe, T. Okada, M. Ueno, T. Mukai, M. Yoshikawa, and J. Kawaguchi, "Itokawa Dust Particles: A Direct Link Between S-Type Asteroids and Ordinary Chondrites," *Science, AAAS*, Vol. 333, 2011, pp. 1113–1116.

[7] J. d. Lafontaine, "Autonomous Spacecraft Navigation and Control for Comet Landing," *J. Guidance, Control and Dynamics*, Vol. 15, No. 3, 1992, pp. 561–576.

[8] B. Açikmeşe, M. Mandić, and L. Blackmore, "Comet GN&C Research Report: G-TAG: A Multibody Simulation Software Testbed for Small Body Exploration and Sampling," *Jet Propulsion Laboratory, JPL D-63133*, 2009.

[9] D. S. Bayard, "Integrated Autonomous Guidance, Navigation and Control for Comet Sample Return: Fiscal Year 2009 RTD Accomplishments Summary," *Jet Propulsion Laboratory, JPL D-63128*, 2009.

[10] B. Açikmeşe, M. Mandić, and L. Blackmore, "Comet GN&C Research Report: G-DYN Version-2: A Multibody Dynamics Engine," *Jet Propulsion Laboratory, JPL D-63132*, 2009.

[11] L. Blackmore, "Comet GN&C Research Report: Six Degree of Freedom Ascent Control for Small Body Touch and Go," *Jet Propulsion Laboratory, JPL D-63134*, 2009.

[12] M. Mandić and B. Açikmeşe, "Comet GN&C Research Report: G-View: A Spacecraft GN&C Visualization Tool for Small Body Exploration and Sampling," *Jet Propulsion Laboratory, JPL D-63138*, 2009.

[13] L. Blackmore, B. Trease, B. Açikmeşe, M. Mandić, and J. M. C. III, "Comet GN&C Research Report: Surface Contact Model for Comets and Asteroids," *Jet Propulsion Laboratory, JPL D-63135*, 2009.